Mathematical Modelling of Transient Processes in a Section of an Electricity Network with Varying Configurations of its Components

Andriy Chaban[1,2,3], Aleksander Dydycz[1,*], Vitaliy Levoniuk[3], Yuriy Biletskyi[2], Ivan Drobot[3]
[1]*Faculty of Transport, Electrical Engineering and Computer Science, Casimir Pulaski Radom University, Malczewskiego St. 26, 26-600 Radom, Poland*
[2]*Institute of Power Engineering and Control Systems, Lviv Polytechnic National University, Bandery St. 12, Lviv, 79000, Ukraine*
[3]*Department of Electrical Systems, Stepan Gzhytskyi National University of Veterinary Medicine and Biotechnologies of Lviv, Pekarska St. 50, Lviv, 79010, Ukraine*
a.chaban@uthrad.pl; [*]a.dydycz@urad.edu.pl; levonyukvr@lnup.edu.ua; yurii.o.biletskyi@lpnu.ua; drobotim@lnup.edu.ua

***Abstract*—This article presents mathematical models of power grid segments. Three load configurations representing real power systems were analysed. The mathematical models were developed using a field-circuit approach. A long line element was considered as a system with distributed parameters. A second-order partial differential equation was used to describe the line. The spatial derivative was discretised using the method of lines. Boundary conditions for the line equation were sought on the basis of circuit approaches. First-order boundary conditions were used. The resulting systems of differential equations were integrated using the implicit Euler method. Using the developed mathematical models, simulations of the behaviour of the systems were carried out. Transient processes during voltage switching were analysed. The results are presented in the form of waveforms of current and voltage at various points on the line. Spatial waveforms of the voltage and current in the line were also prepared.**

***Index Terms*—Mathematical modelling; Distributed parameter systems; Long power transmission line; Boundary conditions.**

I. INTRODUCTION

Mathematical modelling allows for the analysis of the behaviour of energy systems under both normal and emergency conditions. The growing complexity of power networks, particularly those with long transmission lines and varying loads, requires the use of precise models. This challenge is further compounded by the need to use partial differential equations. The difficulty often lies in clearly defining the boundary conditions used for the equations. The form of the conditions depends on the systems at the edges of the lines. In many cases, determining these conditions is difficult or impossible.

The issue remains relevant due to ever-increasing reliability requirements. The high accuracy of mathematical models is essential in the design and analysis of modern systems. Moreover, the growing number of connected Distributed Energy Resources requires a thorough analysis of connection possibilities. Mathematical models are being developed for this purpose.

Mathematical modelling of power grids is an area of global research. We will briefly present publications related to this topic.

The authors in [1] proposed an analytical method for considering steady states in power lines. The developed method uses the Laplace transform. The model was compared with the Π model. Similar research was conducted in [2], whose authors investigated analytical solutions to equations describing induction machines. The models were validated by comparing them with measurements of actual machines under various operating conditions. The results of the experiments were obtained on the basis of the actual parameters of the systems.

In [3], the authors analyse the impact of lightning strikes on transmission lines. Mathematical models with a field approach were used for the analysis. Particular attention was paid to using the concept of moving and accelerating loads when analysing the impact of lightning.

The analysis of long power lines involves considering wave processes. The authors in [4] used a model of a line with distributed parameters and developed differential equations that describe the system. Voltage and current calculations were performed using spline interpolation. The study focussed on analysing the performance of surge arresters in a 500 kV transmission line. The transient processes during line switching were also analysed.

In [5], the authors investigated the use of multicircuit high-voltage lines. The work focusses on the development and use of mathematical models to study transient states in lines. ATP-EMTP software was used to perform the simulations.

The article in [6] is devoted to the analysis of approaches to line modelling. The impact of these approaches on the simulation results was examined. The work was carried out using the ATPDraw graphical environment. The models

Manuscript received 22 April, 2025; accepted 25 June, 2025.

developed were adapted to study transient states in lines with different types of configurations.

The authors in [7], [8] analysed lightning strikes on high-voltage lines. In both articles, ATP-EMTP software was used to simulate the phenomenon. The subject of the analysis was the surges generated in the line. The impact of surge arresters and lightning conductors on the processes on the line was also examined.

In [9], [10], mathematical models of lines were developed using the MATLAB and ATP environments. With presenting a different approach, the impact of lightning strikes was also examined. The analysis covered various lightning scenarios, as well as the impact on return conductors in cable lines. The authors in [9] describe variants of damage to return conductors on a cable line that is part of an overhead and cable network.

Long line theory was also applied in [11], where the authors replaced the inductive element in a buck converter circuit with a long transmission line element. The resulting circuit allows analysis of the power supply when the source and receiver are significantly distant from each other. The research was based on a mathematical model involving a system of differential equations. The results were analysed with the standard model and the model with a long power transmission line.

In [12]–[14], the authors analyse energy systems in the context of distributed energy resources and electric vehicle chargers. System models were constructed using graph theory or GridLab-D software. The research resulted in an analysis of network parameters that accounted for the effects of dynamic load changes. Attention was drawn to voltage drops and voltage instability resulting from the power generated by photovoltaic (PV) installations.

An analysis of the current state of scientific research shows that there are many approaches to modelling energy systems. The authors in [15], [16] discussed the consequences of using modelling software. Ready-made tools in the form of specialised software are often used. However, their use may introduce limitations, such as simplifications of wave processes. Another significant limitation is the difficulty of forming boundary conditions for some systems.

The *aim of this work* is to use field-circuit approaches to develop mathematical models of systems with various configurations.

II. MATHEMATICAL MODEL

In this article, we consider three types of power systems. The main element of the systems discussed is a long power line with distributed parameters. To capture the wave processes that occur in a long line, we use partial differential equations. To simplify the models presented, a single-phase line is considered.

A. System No. 1

To present and derive equations describing the processes in the power supply line, we will use the diagram shown in Fig. 1.

On the basis of the diagram presented, we write down the system of differential equations describing the propagation of current and voltage waves in the line

$$\begin{cases} -\dfrac{\partial u}{\partial x} = R_0 i + L_0 \dfrac{\partial i}{\partial t}, \\ -\dfrac{\partial i}{\partial x} = G_0 u + C_0 \dfrac{\partial u}{\partial t}. \end{cases} \tag{1}$$

This system of equations is known as the telegrapher equations. By differentiating the voltage equation with respect to space and the current equation with respect to time, and substituting one into the other, we obtain from the system of first-order differential equations a single second-order differential equation that describes the propagation of voltage in the line [17]

$$\frac{\partial^2 u}{\partial x^2} = L_0 C_0 \frac{\partial^2 u}{\partial t^2} + \left(L_0 G_0 + R_0 C_0\right)\frac{\partial u}{\partial t} + R_0 G_0 u. \tag{2}$$

By transforming (2) to determine the derivative of the voltage over time, we obtain the following:

$$\begin{aligned} &\frac{\partial v}{\partial t} = \left(L_0 C_0\right)^{-1}\left(\frac{\partial^2 u}{\partial x^2} - \left(L_0 G_0 + R_0 C_0\right)v - R_0 G_0 u\right), \\ &\frac{\partial u}{\partial t} = v, \end{aligned} \tag{3}$$

where u is the voltage in the line, R_0, L_0, C_0, G_0 are the per length parameters of the line, respectively: resistance, inductance, capacitance, conductance per unit length, and v is the time derivative of the voltage.

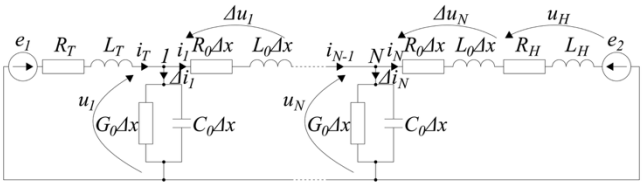

Fig. 1. Calculation diagram for power system No. 1.

By discretising the spatial derivative by the method of lines, using the central scheme, in (2) we eliminated the partial derivative obtaining a system of numerable differential equations for every discretisation node [18]

$$\begin{aligned} \frac{dv_j}{dt} = \frac{u_{j-1} - 2u_j + u_{j+1}}{L_0 C_0 \Delta x^2} - \left(\frac{L_0 G_0 + R_0 C_0}{L_0 C_0}\right)v_j - \\ - \frac{R_0 G_0}{L_0 C_0} u_j, \end{aligned} \tag{4}$$

where Δx is the discrete distance in space and the variable v is defined as

$$\frac{du_j}{dt} = v_j,\ j = 2...N-1. \tag{5}$$

When analysing (4) and (5) for the second discretisation node $j = 2$, it can be seen that it is necessary to determine the voltage u_1. In each of the cases considered, the power line on the left side is connected to the same subsystem consisting of the electromotive force and RL load. This subsystem represents the power system. The voltages u_1 and u_N were

determined using boundary conditions of type I. Analysing the diagram shown in Fig. 1, the equations of stationary connections on the right side of the system were obtained:

$$\begin{cases} i_T - i_1 - \Delta i_1 = 0, \\ \Delta i_1 = \Delta i_{1C} + \Delta i_{1G}, \\ \Delta i_{1G} = G_0 \Delta x u_1, \end{cases} \tag{6}$$

where i_T is the supply current, i_1 is the current in the first discretisation node, and Δi_1 is the leakage current in the first discretisation node.

The unit line capacitance was used to find the voltage at the first discretisation node. Based on (6), the following was obtained

$$\frac{du_1}{dt} = \frac{1}{C_0 \Delta x}\left(i_T - G_0 \Delta x u_1 - i_1\right). \tag{7}$$

Based on Kirchhoff's second law, the input current to the line and the current in the first and penultimate branches of the line discretisation were determined:

$$\frac{di_T}{dt} = \frac{1}{L_T}\left(e_1 - R_T i_T - u_1\right), \tag{8}$$

$$\frac{di_j}{dt} = \frac{1}{L_0 \Delta x}\left(u_j - R_0 \Delta x i_j - u_{j+1}\right);\ j = 1, N-1, \tag{9}$$

where e_1 is the supply voltage and R_T, L_T are the transformer cascade parameters.

The differential equations on the left side of the system will be used in all three load cases considered, because the left side of the system is the same.

Now we write down the equations of stationary connections on the right side of the first system:

$$\begin{cases} i_{N-1} - i_N - \Delta i_N = 0, \\ \Delta i_N = \Delta i_{NC} + \Delta i_{NG}, \\ \Delta i_{NG} = G_0 \Delta x u_N. \end{cases} \tag{10}$$

The voltage at the last node $j = N$ was determined by a similar method to (7)

$$\frac{du_N}{dt} = \frac{1}{C_0 \Delta x}\left(i_{N-1} - G_0 \Delta x u_N - i_N\right). \tag{11}$$

This equation includes the current i_N, which we determine using Kirchoff's second law [17]

$$\frac{di_N}{dt} = \frac{1}{L_0 \Delta x + L_H}\left(u_N - \left(R_0 \Delta x + R_H\right) i_N - e_2\right), \tag{12}$$

where R_H, L_H are the load parameters and e_2 is the voltage source from the other end of the line.

The following system of equations is subject to joint integration (4), (5), (7)–(9), (11), (12).

B. System No. 2

Figure 2 shows a diagram of the power system considered in the second case.

The left side of the circuit remains the same, while on the right side, the RL load is presented as a cascade of transformers followed by four branches of the following types: R, RL, RLC, and L. The branches represent a set of loads of various types connected to the secondary winding of the last transformer.

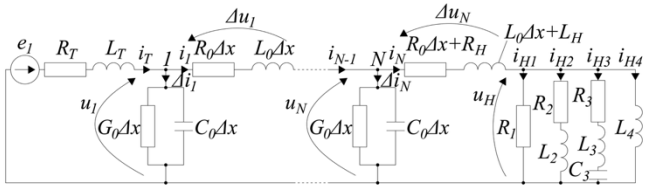

Fig. 2. Calculation diagram for power system No. 2.

The equations describing the left side of the system remain the same, while for the right side we first write down the equations of stationary connections based on Kirchhoff's first law

$$\begin{aligned} &i_N - i_{H1} - i_{H2} - i_{H3} - i_{H4} = 0 \Rightarrow \\ &\Rightarrow i_N - i_{H2} - i_{H3} - i_{H4} = i_{H1}, \end{aligned} \tag{13}$$

where i_N is the current in the last discretisation node and i_{H1}, i_{H2}, i_{H3}, i_{H4} are the currents in load branches.

To find the load voltage, we use branch R. To determine the required voltage, we write Ohm's law taking into account (13)

$$u_H = \left(i_N - i_{H2} - i_{H3} - i_{H4}\right) R_1, \tag{14}$$

where u_H is the voltage at the end of the line and R_1 is the resistance in the first load branch.

Now, based on the diagram in Fig. 2, we will write down the equations to find the currents in individual load branches [19]:

$$\frac{di_N}{dt} = \frac{1}{L_0 \Delta x + L_H}\left(u_N - \left(R_0 \Delta x + R_H\right) i_N - u_H\right), \tag{15}$$

$$\frac{di_{H2}}{dt} = \frac{1}{L_2}\left(u_H - R_2 i_{H2}\right), \tag{16}$$

$$\begin{cases} \dfrac{di_{H3}}{dt} = \dfrac{1}{L_3}\left(u_H - R_3 i_{H3} - u_{C3}\right), \\ \dfrac{du_{C3}}{dt} = \dfrac{i_{H3}}{C_3}, \end{cases} \tag{17}$$

$$\frac{di_{H4}}{dt} = \frac{u_H}{L_4}, \tag{18}$$

where R_H, L_H are the transformer cascade parameters and R_2, L_2, R_3, L_3, C_3, L_4 are the load branches parameters.

To describe the behaviour of the system shown in Fig. 2, the following system of equations is subject to joint integration: (4), (5), (7)–(9), (11), (15)–(18), taking into account (14).

C. System No. 3

Figure 3 shows the third power system considered.

As in previous cases, the left side remains unchanged. On the right side, the system is loaded with an RL type as a

cascade of transformers and, in parallel, with a capacitance C representing reactive power compensation. An electromotive force is connected in series behind the parallel branches. The whole represents another branch of the power system with reactive power compensation.

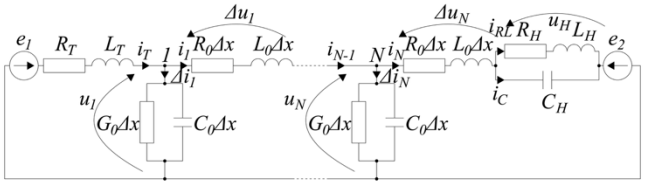

Fig. 3. Calculation diagram for power system No. 3.

To determine the current at the end of the line, the equations of steady-state connections were obtained based on Fig. 3

$$i_N - i_{RL} - i_C = 0 \Rightarrow i_C = i_N - i_{RL}, \tag{19}$$

where i_{RL}, i_C are the currents in the load branches.

Proceeding in the same manner as in the previous points, the equation was recorded to determine the current in the load [15]

$$\frac{di_N}{dt} = \frac{1}{L_0 \Delta x}\left(u_N - R_0 \Delta x i_N - u_H - e_2\right). \tag{20}$$

The current in the RL load branch was sought using Kirchhoff's second law. The following equation describing the behaviour of the current in the RL branch was obtained

$$\frac{di_{RL}}{dt} = \frac{1}{L_H}\left(u_H - R_H i_{RL}\right). \tag{21}$$

The load voltage was sought using the C_H capacity. The result is the following equation

$$\frac{du_H}{dt} = \frac{1}{C_H}\left(i_N - i_{RL}\right), \tag{22}$$

where C_H is the load branch capacity.

To describe the behaviour of the system shown in Fig. 3, the following equations are subject to joint integration: (4), (5), (7)–(9), (11), (20)–(22).

III. COMPUTER SIMULATION

The computer simulation was performed using the parameters of actual power systems. The power supply from a turbo generator was assumed to be an ideal voltage source, via a block transformer, and then via a step-up transformer. This subsystem was represented as the electromotive force e_1 and the loads R_T and L_T representing the transformers. The next element is a long power line. Line load was considered as three types of power system.

The simulation considered an actual transmission line with a rated voltage of 750 kV. Line parameters used in the simulation: $L = 476$ km, $R_0 = 1.9 \cdot 10^{-5}$ Ω/km, $L_0 = 9.24 \cdot 10^{-7}$ H/km, $C_0 = 1.32 \cdot 10^{-11}$ F/km, $G_0 = 3.2 \cdot 10^{-11}$ S/km. The line considered was divided into 40 discretisation nodes, so that the distance $\Delta x = 11{,}9$ km.

Load parameters: $R_H = 400$ Ω, $L_H = 0{,}8$ H, $C_H = 1$ μF, $R_1 = 1200$ Ω, $R_2 = 800$ Ω, $L_2 = 0.64$ H, $R_3 = 600$ Ω, $L_3 = 0.32$ H, $C_3 = 5$ μF, $L_4 = 5$ H.

Parameters of the represented energy subsystems: $e_1 = 623 \cdot 10^3 \cdot \sin(\omega t)$ V, $e_2 = 623 \cdot 10^3 \cdot \sin(\omega t + 29.2°)$ V, $R_T = 3.1$ Ω, $L_T = 0.29$ H.

The presented systems of differential equations were solved using the implicit Euler method with fixed-point iteration.

Figure 4 shows the voltage waveform in system No. 1 at the penultimate discretisation node. During line switching, a transient state occurs, causing the voltage to rise and fall. After approximately 0.08 s, the processes reach a steady state. The voltage value is higher than the set value.

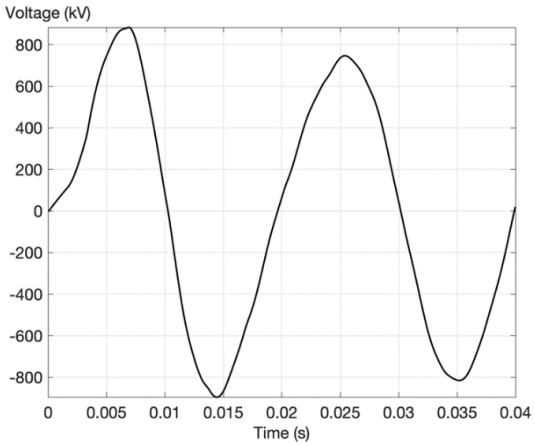

Fig. 4. Voltage waveform on 464 km of line in system No. 1.

Figure 5 shows the current waveform in the penultimate discretisation node of the line. At $t = 0.01$ s, the current reaches a value close to 1 kA. In steady state, the current value is approximately 690 A.

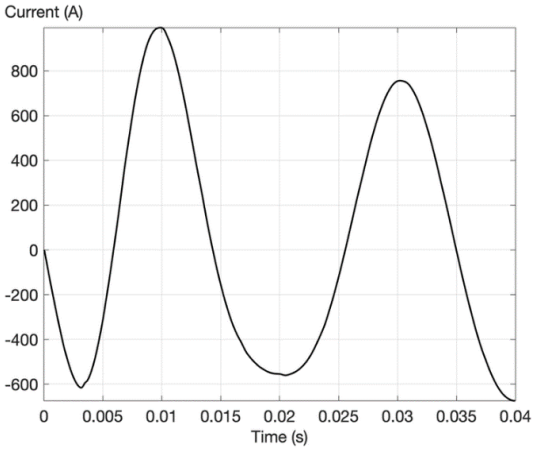

Fig. 5. Current waveform on 464 km of line in system No. 1.

Figure 6 shows the voltage waveform in system No. 2 at the penultimate discretisation node. The figure shows a faster transition to steady state compared to system No. 1. The peak voltage value is also significantly lower.

Figure 7 shows the current waveform at the penultimate discretisation node of the line. The initial current value is lower than the steady-state value.

The presented waveforms differ from those characterising system No. 1. First, they are milder in nature and have shorter

transition processes. This is due to the nature of system No. 2, namely that this system is only a representation of the load ensemble. In system No. 1, the electromotive force on both sides of the line was taken into account. This is a representation of distributed power generation. Therefore, in system No. 1, voltage sources appear at both ends of the line, resulting in more dynamic processes.

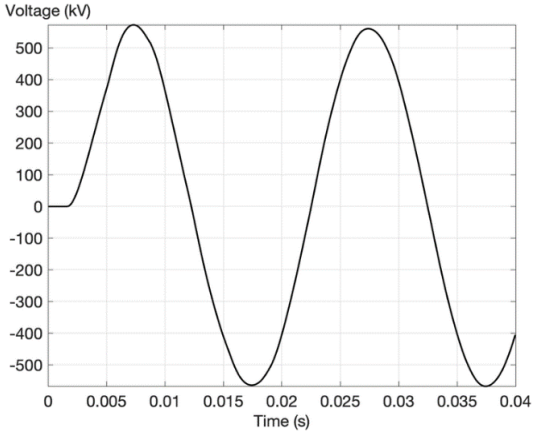

Fig. 6. Voltage waveform on 464 km of line in system No. 2.

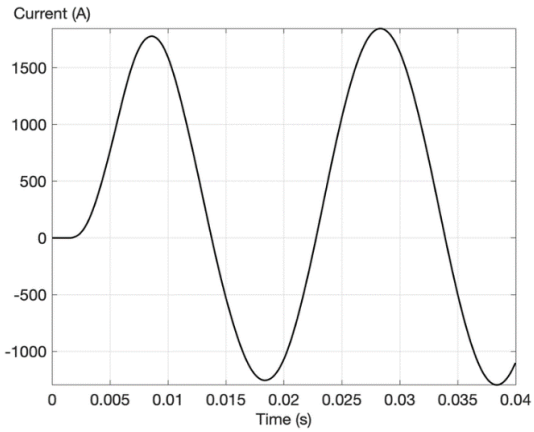

Fig. 7. Current waveform on 464 km of line in system No. 2.

Figure 8 shows the voltage waveform at the last discretisation node in system No. 3. This system differs from system No. 1 only by adding a compensation battery. The other parameters remain unchanged. The dynamic transient states of the voltage are clearly visible in comparison to the waveform in Fig. 4.

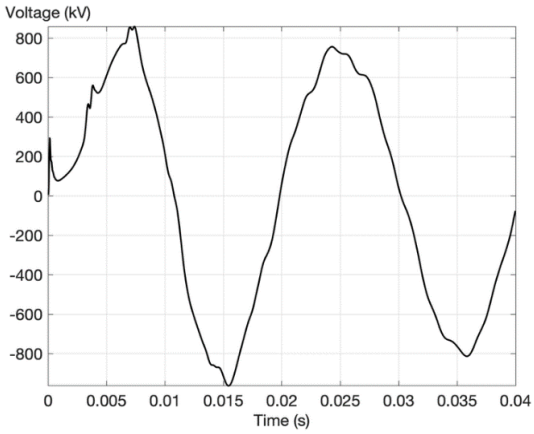

Fig. 8. Voltage waveform on 464 km of line in system No. 3.

Figure 9 shows the current waveform in a 464 km line. Once again, significant differences can be observed in comparison to the current flow in system No. 1. The system reaches a steady state after 0.15 s. The highest current value in the transient state reached 1224 A. In steady state, the current value is 688 A.

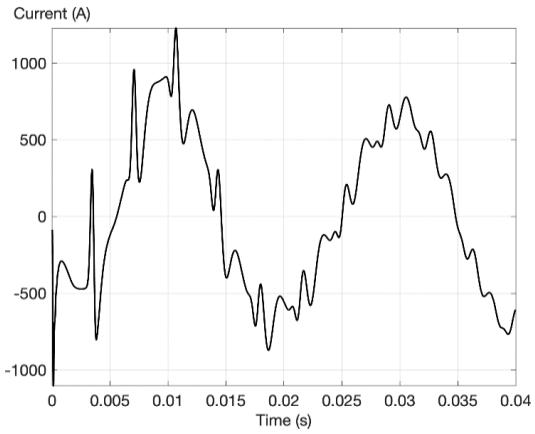

Fig. 9. Current waveform on 464 km of line in system No. 3.

Figure 10 shows the spatial distribution of voltage and current in system No. 1 at time *t = 0.0031 s*. The graph shows slight distortions in both the current and voltage waveforms.

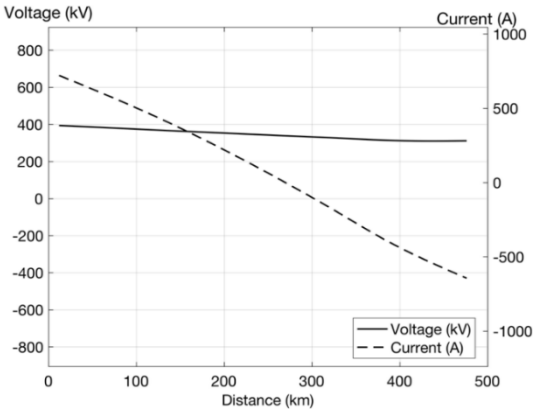

Fig. 10. Spatial distribution of current and voltage in system No. 1 at time *t = 0.0031 s*.

Figure 11 shows the spatial distribution of voltage and current in system No. 2 at time *t = 0.0031 s*. Compared to the distribution shown in Fig. 10, a smaller phase-shift angle between the current and voltage is observed.

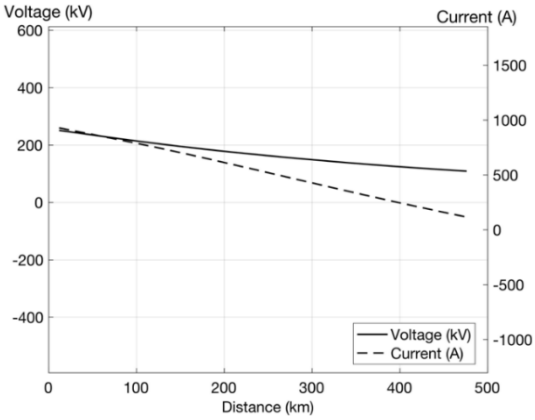

Fig. 11. Spatial distribution of current and voltage in system No. 2 at time *t = 0.0031 s*.

Figure 12 shows the spatial voltage and current waveforms in line 3 at time *t = 0.0031 s*. The influence of wave processes in the line on the shape of the current and voltage waveforms

is clearly visible. In the distribution shown in Fig. 12, current and voltage waves moving between the line terminals were observed. The dynamics of wave processes depend on the characteristic impedance of the line and the impedance at its edges.

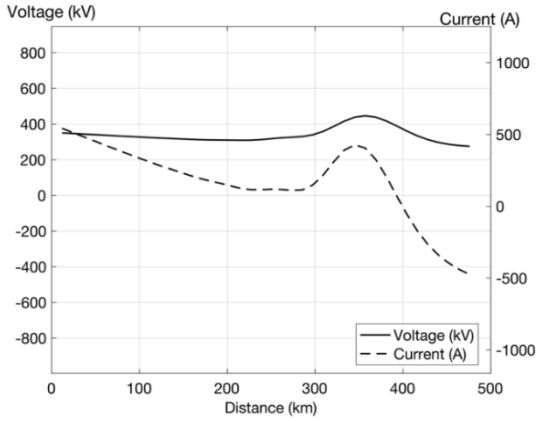

Fig. 12. Spatial distribution of current and voltage in system No. 3 at time $t = 0.0031$ *s*.

By comparing Figs. 10 and 12, similar current and voltage values can be observed at the ends of the intervals. A significant difference is the appearance of current and voltage waves as a result of the addition of a capacitive element. This is due to a change in the termination impedance. It is also important to match the value and nature of the impedance at the ends with the characteristic impedance of the line.

Figures 13–15 show the temporal and spatial voltage waveforms in individual systems during the time $t \in (0; 0.04)$ s.

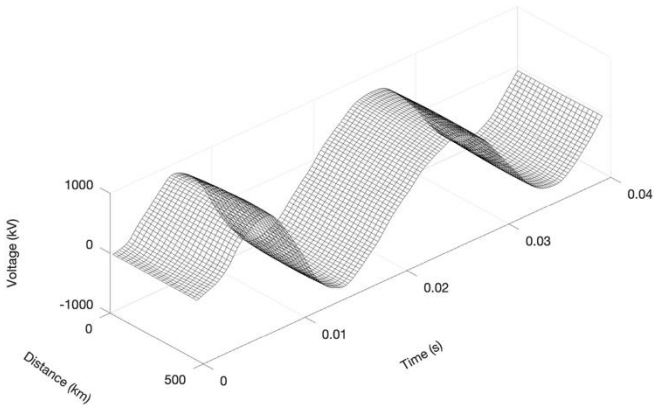

Fig. 13. The temporal-spatial waveform of voltage in system No. 1 in time $t \in (0; 0.04)$ *s*.

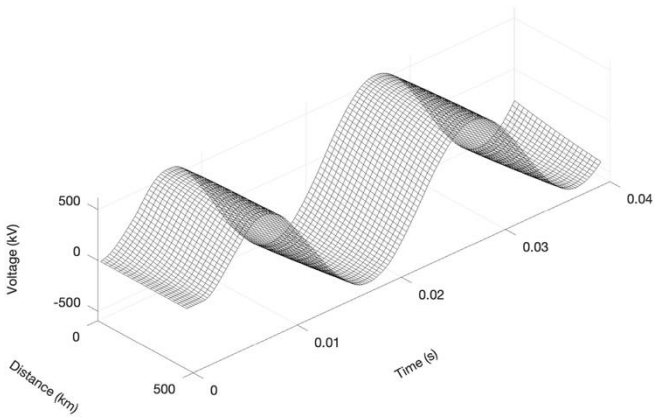

Fig. 14. The temporal-spatial waveform of voltage in system No. 2 in time $t \in (0; 0.04)$ *s*.

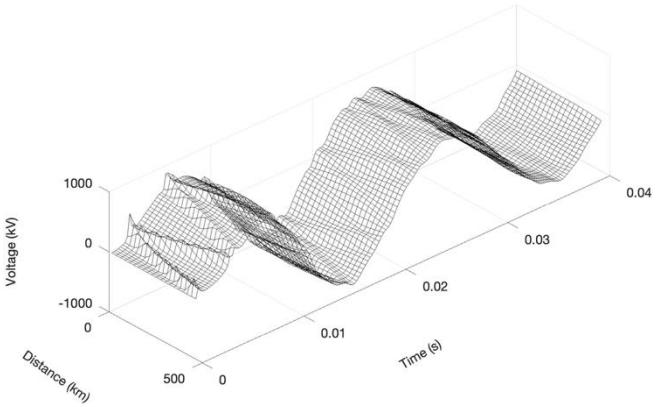

Fig. 15. The temporal-spatial waveform of voltage in system No. 3 in time $t \in (0; 0.04)$ *s*.

The waveforms in Figs. 13 and 14 are similar, gentle in nature, and smooth. Only gentle voltage waves passing between line terminations can be observed. The waveform in Fig. 15 clearly indicates intense wave processes occurring in the line. A voltage wave is generated, reflecting off-line terminations. The travelling wave exhibits a time-attenuated character.

The use of time-space waveforms facilitates the analysis of processes occurring on the line. The deformations and behaviour of electromagnetic waves are more clearly visible in the waveforms. This facilitates the analysis of wave dynamics in relation to time and space.

IV. CONCLUSIONS

The mathematical models developed enable the analysis of real energy systems with various popular configurations.

The use of circuit approaches to determine the boundary conditions of the telegrapher equation is sufficient to model typical power systems.

On the basis of the results of computer simulations, the impact of load impedance on wave processes can be observed. The impact of energy sources on the stability of power grids can also be seen.

Using the concepts presented, it is possible to develop mathematical models describing power compensation in systems with a large number of distributed sources. The extension of the concept to three-phase systems also remains an open question. The possibility of using overhead HVDC networks in parallel with existing HVAC networks can also be considered.

CONFLICTS OF INTEREST

The authors declare that they have no conflicts of interest.

REFERENCES

[1] S. H. L. Cabral, S. F. Stefenon, R. G. Ovejero, and V. R. Q. Leithardt, "Practical validation of a new analytical method for the analysis of power transmission lines at steady state", *IEEE Access*, vol. 11, pp. 87667–87675, 2023. DOI: 10.1109/ACCESS.2023.3303410.

[2] I. Knezevic, M. Calasan, T. Dlabac, F. Filipovic, and N. Mitrovic, "Exact analytical solutions for modelling the speed-time characteristics of direct-start induction machines under various operational conditions on ships: Review and experimental validation", *Elektronika ir Elektrotechnika*, vol. 30, no. 6, pp. 4–12, 2024. DOI: 10.5755/j02.eie.38518.

[3] T. Cakil, H. F. Carlak, and S. Ozen, "The indirect effect of lightning electromagnetic pulses on electrostatic, electromagnetic fields and induced voltages in overhead energy transmission lines", *Applied Sciences*, vol. 14, no. 7, p. 3090, 2024. DOI: 10.3390/app14073090.

[4] R. Huseyn, A. M. Hashimov, A. Shokri, and H. Mukalazi, "Calculation algorithm for electromagnetic wave processes in multi-wire intersystem ETL", *Discover Electronics*, vol. 1, art. no. 5, 2024. DOI: 10.1007/s44291-024-00005-2.

[5] D. Zychma and P. Sowa, "Electromagnetic transients in multi-voltage transmission lines during non-simultaneous faults", *Energies*, vol. 15, no. 3, p. 1046, 2022. DOI: 10.3390/en15031046.

[6] T. P. dos Reis and A. Raizer, "Modeling and simulation of distribution networks under lightning transients: A comparative study of accuracy and complexity", *Energies*, vol. 17, no. 2, p. 337, 2024. DOI: 10.3390/en17020337.

[7] S. Boumous, Z. Boumous, and Y. Djeghader, "The impact of lightning strike on hybrid high voltage overhead transmission line - Insulated gas line", *Informatyka, Automatyka, Pomiary w Gospodarce i Ochronie Środowiska*, vol. 14, pp. 27–31, 2024. DOI: 10.35784/iapgos.5445.

[8] S. Boumous, Z. Boumous, Z. Anane, and H. Nouri, "Comparative study of 220 kV overhead transmission lines models subjected to lightning strike simulation by using electromagnetic and alternative transients program", *Electrical Engineering & Electromechanics*, vol. 4, pp. 68–74, 2022. DOI: 10.20998/2074-272X.2022.4.10.

[9] R. Tarko, J. Gajdzica, W. Nowak, and W. Szpyra, "Study of the lightning overvoltage protection effectiveness of high voltage mixed overhead cable power lines", *Energies*, vol. 14, no. 8, p. 2329, 2021. DOI: 10.3390/en14082329.

[10] J. A. Morales, G. D. Guidi Venerdini, and B. M. Keune, "Dynamic simulation of lightning strikes on transmission lines based on ATP-MATLAB", *International Journal of Applied Engineering Research*, vol. 10, pp. 34390–34395, 2015.

[11] K. Röbenack and D. Gerbet, "Current-mode control of a distributed buck converter with a lossy transmission line", *Electronics*, vol. 13, no. 17, p. 3565, 2024. DOI: 10.3390/electronics13173565.

[12] A. Hamza, S. T. H. Rizvi, M. U. Safder, and H. Asif, "A novel mathematical approach to model multi-agent-based main grid and microgrid networks for complete system analysis", *Machines*, vol. 10, no. 2, p. 110, 2022. DOI: 10.3390/machines10020110.

[13] M. Tomasov, D. Motyka, M. Kajanova, and P. Bracinik, "Modelling effects of the distributed generation supporting e-mobility on the operation of the distribution power network", *Transportation Research Procedia*, vol. 40, pp. 556–563, 2019. DOI: 10.1016/j.trpro.2019.07.080.

[14] V. Blazek *et al.*, "A novel approach to utilization vehicle to grid technology in microgrid environment", *International Journal of Electrical Power & Energy Systems*, vol. 158, art. 109921, pp. 1–17, 2024. DOI: 10.1016/j.ijepes.2024.109921.

[15] A. Chaban, A. Popenda, A. Szafraniec, and V. Levoniuk, "Including shield wires in the analysis of transient processes occurring in HVAC transmission lines", *Energies*, vol. 16, no. 23, p. 7870, 2023. DOI: 10.3390/en16237870.

[16] F. Rachidi, "A review of field-to-transmission line coupling models with special emphasis to lightning-induced voltages on overhead lines", *IEEE Transactions on Electromagnetic Compatibility*, vol. 54, no. 4, pp. 898–911, 2012. DOI: 10.1109/TEMC.2011.2181519.

[17] A. Chaban, *Hamilton-Ostrogradski Principle in Electromechanical Systems*. Soroki: Lviv, Ukraine, 2015.

[18] T. Perzyński, V. Levoniuk, and R. Figura, "Transient electromagnetic processes analysis in high voltage transmission lines during two-phase short circuits", *Sensors*, vol. 23, no. 1, p. 298, 2023. DOI: 10.3390/s23010298.

[19] X. Dai, J. Zhai, Y. Jiang, Y. Guo, C. N. Jones, and V. Hagenmeyer, "Advancing distributed AC optimal power flow for integrated transmission-distribution systems", *IEEE Transactions on Network Science and Engineering*, vol. 12, no. 2, pp. 1210–1223, 2025. DOI: 10.1109/TNSE.2025.3526206.